Noninvasive Measurement of Cerebral Blood Flow and Blood Oxygenation Using Near-Infrared and Diffuse Correlation Spectroscopies in Critically Brain-Injured Adults

Meeri N. Kim · Turgut Durduran · Suzanne Frangos · Brian L. Edlow ·
Erin M. Buckley · Heather E. Moss · Chao Zhou · Guoqiang Yu ·
Regine Choe · Eileen Maloney-Wilensky · Ronald L. Wolf · M. Sean Grady ·
Joel H. Greenberg · Joshua M. Levine · Arjun G. Yodh · John A. Detre ·
W. Andrew Kofke

Abstract

Background This study assesses the utility of a hybrid optical instrument for noninvasive transcranial monitoring in the neurointensive care unit. The instrument is based on diffuse correlation spectroscopy (DCS) for measurement of cerebral blood flow (CBF), and near-infrared spectroscopy (NIRS) for measurement of oxy- and deoxy-hemoglobin concentration. DCS/NIRS measurements of CBF and oxygenation from frontal lobes are compared with concurrent xenon-enhanced computed tomography (XeCT) in patients during induced blood pressure changes and carbon dioxide arterial partial pressure variation.

Methods Seven neurocritical care patients were included in the study. Relative CBF measured by DCS ($rCBF_{DCS}$), and changes in oxy-hemoglobin (ΔHbO_2), deoxy-hemoglobin (ΔHb), and total hemoglobin concentration (ΔTHC), measured by NIRS, were continuously monitored throughout XeCT during a baseline scan and a scan after intervention. CBF from XeCT regions-of-interest (ROIs) under the optical probes were used to calculate relative XeCT CBF ($rCBF_{XeCT}$) and were then compared to $rCBF_{DCS}$. Spearman's rank coefficients were employed to test for associations between $rCBF_{DCS}$ and $rCBF_{XeCT}$, as well as between rCBF from both modalities and NIRS parameters.

Results $rCBF_{DCS}$ and $rCBF_{XeCT}$ showed good correlation ($r_s = 0.73$, $P = 0.010$) across the patient cohort. Moderate correlations between $rCBF_{DCS}$ and $\Delta HbO_2/\Delta THC$ were also observed. Both NIRS and DCS distinguished the effects of xenon inhalation on CBF, which varied among the patients.

Conclusions DCS measurements of CBF and NIRS measurements of tissue blood oxygenation were successfully obtained in neurocritical care patients. The potential for DCS to provide continuous, noninvasive bedside

M. N. Kim (✉) · T. Durduran · E. M. Buckley · C. Zhou ·
G. Yu · R. Choe · A. G. Yodh
Department of Physics and Astronomy, University
of Pennsylvania, 209 South 33rd Street, Philadelphia,
PA 19104, USA
e-mail: meeri@sas.upenn.edu

T. Durduran · R. L. Wolf · J. A. Detre
Department of Radiology, University of Pennsylvania,
Philadelphia, PA, USA

S. Frangos · E. Maloney-Wilensky · M. S. Grady ·
J. M. Levine · W. A. Kofke
Department of Neurosurgery, University of Pennsylvania,
Philadelphia, PA, USA

B. L. Edlow · H. E. Moss · J. H. Greenberg ·
J. M. Levine · J. A. Detre
Department of Neurology, University of Pennsylvania,
Philadelphia, PA, USA

J. M. Levine · W. A. Kofke
Department of Anesthesiology and Critical Care, University
of Pennsylvania, Philadelphia, PA, USA

T. Durduran
ICFO—Institut de Ciències Fotòniques, Mediterranean
Technology Park, 08860 Castelldefels, Barcelona, Spain

G. Yu
Center for Biomedical Engineering, University of Kentucky,
Lexington, KY, USA

monitoring for the purpose of CBF management and individualized care is demonstrated.

Introduction

Measurement of cerebral blood flow (CBF) provides valuable information for clinical management of neuro-critical care patients, but current modalities for monitoring CBF are often limited by practical and technological hurdles. Such hurdles include cost, exposure to ionizing radiation, and the logistical challenges and increased risk to critically ill patients when transportation out of the neu-rointensive care unit is required [1]. Furthermore, standard radiological modalities such as CT, PET, and MRI cannot provide continuous measures of CBF that may be required in clinically unstable patients. Bedside techniques for monitoring CBF include transcranial Doppler (TCD) ultrasonography [2], and thermal diffusion [3] and laser Doppler flowmetries [4]. However, TCD ultrasonography is limited to observations of large vessel flow velocities, which do not necessarily reflect microvascular perfusion in patients with cerebrovascular disease [5], and both thermal diffusion and laser Doppler flowmetries are invasive.

Diffuse correlation spectroscopy (DCS) is a novel non-invasive optical technique with potential as an alternative approach for bedside CBF monitoring. DCS uses near-infrared light within the therapeutic spectral window (i.e., wavelengths from ~ 650 to ~ 950 nm) to provide a con-tinuous, transcranial measure of blood flow. Changes in blood flow are obtained from DCS by measuring the decay rate of the detected light intensity autocorrelation function (g_2) [6–8]. At present, quantitative absolute measurements of CBF with DCS are difficult to obtain, and thus we typically derive microvascular relative CBF ($rCBF_{DCS}$), i.e., blood flow changes relative to some baseline period. Near-infrared spectroscopy (NIRS) is a more widely known optical monitoring technique that derives concen-tration changes of oxy- and deoxy-hemoglobin (ΔHbO_2, ΔHb) [9, 10]. In this study, we have integrated DCS with NIRS in a hybrid optical instrument that simultaneously monitors CBF and oxy- and deoxy-hemoglobin concen-trations. The instrument thus facilitates monitoring both CBF and oxygen metabolism in neurocritical care patients. The continuous and noninvasive nature of these optical techniques may lead to new clinical tools in the neurointensive care unit.

NIRS and, more recently, DCS have been employed to measure tissue perfusion and oxygenation in human populations. For example, NIRS/DCS has detected changes in autoregulatory function associated with ischemic stroke [11] and healthy aging [12]. $rCBF_{DCS}$ measurements also have been validated against fluorescent microspheres in brain-injured piglets [13]. This study is the first to evaluate $rCBF_{DCS}$ in an adult neurocritical care population.

In this preliminary study, we assessed the feasibility of DCS as a continuous monitor of CBF in neurocritical care patients by comparing DCS measurements of CBF with a more established technique, stable xenon-enhanced CT (XeCT) [14, 15]. XeCT is a diffusible tracer technique that provides quantitative CBF by administering xenon via inhalation and using the time-dependent concentration of xenon in tissue as a measure of perfusion. XeCT CBF calculations are based on the modified Kety-Schmidt equation, which describes the relationship of CBF to the tracer blood/brain partition coefficient and tracer concen-tration in the brain and arterial blood [16]. We performed continuous bedside NIRS/DCS with two serial concurrent XeCT measurements in a cohort of patients in whom pharmacological or physiological interventions aimed at altering CBF were administered. We hypothesized that $rCBF_{DCS}$ would correlate with CBF measured by XeCT in co-registered spatial regions of the injured brain, and that correlations would also exist between CBF measured by both techniques and NIRS parameters.

Methods

Patients were considered eligible for study enrollment if they were ≥18 years old and were receiving care in the Hospital of the University of Pennsylvania neurointensive care unit for aneurysmal subarachnoid hemorrhage, trau-matic brain injury, or ischemic stroke. Patients were recruited through the Department of Neurology and the Neurosurgery Clinical Research Division under a research protocol for the study of portable xenon-enhanced CT. Written consent for both the XeCT and optical monitoring portions of the study was provided by the subject (if able) or by a legally authorized representative. All studies were conducted in the patient's room, following protocols approved by the University of Pennsylvania Institutional Review Board.

As part of routine neurocritical care, a variety of physio-logic parameters were monitored throughout the duration of the study. Intracranial pressure (ICP) was monitored either by an external ventricular device or a fiberoptic intraparen-chymal catheter (Camino-MPM1; Integra NeuroSciences, Plainsboro, NJ). Cerebral perfusion pressure (CPP) was calculated from the difference between mean arterial pres-sure (MAP), measured by an arterial line, and ICP.

NIRS/DCS

The hybrid diffuse optical device used in this study contains both DCS and NIRS modules. The DCS module uses two long-coherence-length, continuous-wave 785 nm lasers (CrystaLaser Inc., Reno, NV) for sources, eight photon-counting fast avalanche photodiodes (Perkin Elmer, Canada) for detection, and two 4-channel autocorrelator boards (Correlator.com, Bridgewater, NJ) to compute g_2. The NIRS module employs three wavelengths of amplitude-modulated near-infrared light (685, 785, and 830 nm) for sources, and two photomultiplier tubes for detection. The probe held four optical fibers (one source and detector each for DCS/NIRS) at a fixed configuration (Fig. 1, inset) to permit the two optical modalities to measure nearly concurrent changes in approximately the same volume of tissue. The source–detector separation was 2.5 cm, and the depth of penetration of light into tissue was approximately 1.25–1.5 cm. As shown in Fig. 1, perturbations from voxels within the darkest banana-shaped region (about 1.25 cm deep) have the greatest influence on the detected optical signal, with lighter regions having progressively less influence. This penetration depth permits the near-infrared light to interrogate microvasculature within the surface region of adult cerebral cortex [17].

Optical probes were positioned on both sides of the forehead, over the left and right frontal poles. $rCBF_{DCS}$, ΔHbO_2, ΔHb, and ΔTHC for each hemisphere were updated every 7 s. Positioning and shielding of the probes were adjusted until adequate signal was confirmed prior to data collection. In one instance, optical data could not be obtained; this patient had traumatic epidural and subdural hematomas along the anterior bifrontal convexities. These particular hematomas prevented sufficient photon
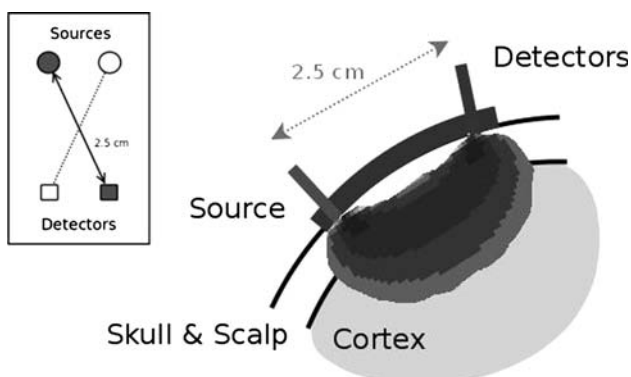

Fig. 1 *Right:* Schematic of the source–detector separation of the optical probe. The resulting area of highest probability signal origin is shown as dark gray, with the lighter areas having lower probability of signal. *Left:* Schematic of optical probe, with DCS/NIRS source–detector pairs in crossed configuration at a fixed separation of 2.5 cm to measure approximately same volume of tissue

transmission through the cortex due to excessive absorption by the concentrated blood.

DCS data analysis used a Brownian diffusion model to characterize relative blood flow [7, 8], along with a semi-infinite, homogeneous medium model for the optical properties of the head to fit the measured autocorrelation functions [18]. Decay curves that failed to fit the model produced low confidence results and were omitted from the analysis. A modified Beer–Lambert law was used for NIRS analysis [19]. Details of both DCS and NIRS analyses have been published previously [20, 21].

Stable Xenon-Enhanced CT

Xenon CT studies were performed with a portable CT scanner (Neurologica Ceretom®) and a stable xenon delivery circuit using the following parameters: inhalation of 28% xenon mixed with oxygen, 100 kV/5–6 mA CT parameters, low dose resolution (2 s scan), 8 time points (2 during baseline and 6 during xenon administration), 6 imaging locations (two 1 cm images per 2 s scan), and estimated dose CTDIw = 120 mGy (CereTom portable CT scanner, Neurologica, Danvers, MA). Six adjacent 10-mm-thick axial quantitative CBF maps (along with their respective confidence maps) were generated using product software (Xenon-CT System 2, Diversified Diagnostic Products Inc, Houston, TX) to derive blood flow (ml/100 g brain/min) for each voxel of the CT image [15, 22–24].

The XeCT scans were used clinically to evaluate the effect of a physiological intervention on CBF, e.g., manipulation of MAP or arterial partial pressure of carbon dioxide. The specific intervention performed was at the discretion of the attending neurointensivist and varied depending on the particular clinical scenario. For example, if regions of oligemia were observed on the baseline XeCT, then MAP was increased by approximately 20% by administering increased doses of vasopressors. If regions of hyperemia were observed, then vasopressor dose was lowered, antihypertensive medications were administered, or ventilation rate was increased. A second XeCT scan was then performed after a minimum of 10 min to re-evaluate CBF after the intervention.

Regions-of-interest (ROIs) of approximately 6–8 ml from the CBF_{XeCT} images, corresponding to the regions of cerebral cortex under the optical probes, were chosen by a physician blinded to the optical results. Figure 2 shows a representative noncontrast CT image slice where optical probes can be seen on the forehead, with outlined ROIs on the corresponding CBF map. ROIs with greater than 30% of pixels having motion artifact or beam-hardening artifact, e.g., due to surgical staples or monitoring equipment, were identified by visual inspection and excluded from the analysis [25].
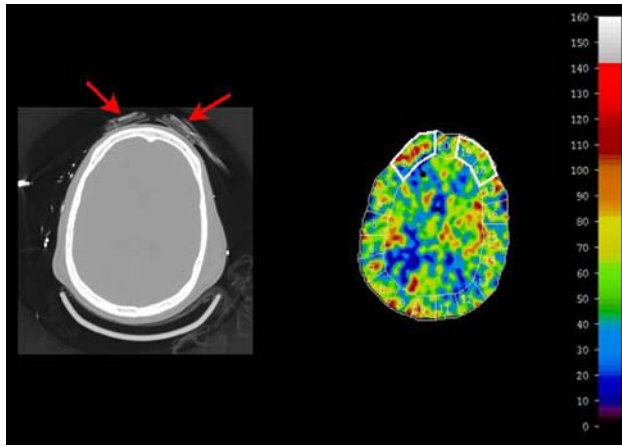
Fig. 2 *Left*: Representative axial slice from bone-windowed, non-contrast CT scan (Pt. 7) showing optical probes on both sides of the forehead (*arrows*). *Right*: CBF map from XeCT baseline scan of the same axial slice with ROIs under DCS/NIRS probes outlined

Statistical Analysis

For each ROI, the change in relative CBF_{XeCT} ($rCBF_{XeCT}$) was calculated as the percentage change from the baseline scan: $rCBF_{XeCT} = (CBF_{XeCT,IN} - CBF_{XeCT,BL})/CBF_{XeCT,BL}$. Here $CBF_{XeCT,IN}$ refers to absolute CBF_{XeCT} measured after intervention from the second scan, and $CBF_{XeCT,BL}$ is absolute CBF_{XeCT} from the baseline scan. All continuous time-series data (NIRS/DCS/MAP) were computed using the average ($< >$) of the 2-min period prior to xenon administration for both baseline (Δt_{BL}) and intervention (Δt_{IN}) XeCT scans: $rCBF_{DCS} = [<rCBF_{DCS}(\Delta t_{IN})> - <rCBF_{DCS}(\Delta t_{BL})>]/<rCBF_{DCS}(\Delta t_{BL})>$. The changes $\Delta HbO_2/\Delta Hb/\Delta tHC/\Delta MAP$ were defined as $\Delta Y = <Y(\Delta t_{IN})> - <Y(\Delta t_{BL})>$, with Y representing the parameter of interest. The period prior to xenon administration was used to exclude the possible effects of hemodynamic change due to pharmacological effects of xenon gas [26].

Spearman's rank coefficients were used to assess various correlations between $rCBF_{XeCT}$, $rCBF_{DCS}$, ΔHbO_2, ΔHb, and ΔTHC. To analyze the effects of xenon wash-in on CBF, a paired Student's *t*-test was used to compare population-averaged CBF from the minute before xenon inhalation had begun to population-averaged CBF at the time that xenon had fully washed in (6 min after start of inhalation).

Results

Clinical and study data for the 10 episodes of measurement are provided in Table 1. The eight patients (five males/three females) had a mean age of 48 years (range, 18–82 years). The Glasgow Coma Score (GCS) ranged from 3 to 15 on admission, and from 3 to 9 on the day of measurement, while study timing ranged from ICU day 2 to 9. Interventions included decrease in vasopressor medication dose (four patients), increase in vasopressor medication dose (two patients), increase in ventilator respiratory rate (one patient), and increase in antihypertensive medication dose (one patient). Pharmacological and physiological interventions are summarized in Table 1.

Comparisons between XeCT and NIRS/DCS parameters were performed using at least one ROI from seven patients (due to poor XeCT confidence, thus exclusion, for both ROIs in Pt. 5), while comparisons between NIRS and DCS parameters were performed using data from all eight patients. Changes in MAP, CPP, CBF_{XeCT}, and DCS data for baseline and intervention measurements with sufficient confidence are presented in Table 2.

Comparison of $rCBF_{XeCT}$ and $rCBF_{DCS}$/NIRS Data

Changes in CBF measured by DCS and XeCT were in good agreement. Figure 3 shows the observed correlation ($r_s = 0.73$, $P = 0.010$), indicating a positive and significant association between $rCBF_{XeCT}$ and $rCBF_{DCS}$. The linear fit by simple regression has a slope equal to 1.1, with an offset of 9.3%. ΔHbO_2 was moderately correlated with $rCBF_{XeCT}$ and bordered on significance ($r_s = 0.57$, $P = 0.053$).

Table 1 Patient clinical and study data	No.	Gender	Age	Injury	Initial GCS	Study GCS	Intervention
	1	F	62	SAH	15	8	Phenylephrine ↓
	2	M	18	TBI	3	7	Ventilator respiratory rate ↑
	3	M	23	AIS	7	3	Labetalol ↑
	4	M	46	SAH	14–15	6	Norepinephrine ↑
	5	M	38	SAH	15	9	Phenylephrine ↑
	6	M	82	TBI	11	6	Norepinephrine ↓
	7-1	F	50	SAH	3	3	Norepinephrine ↓, Phenylephrine ↓
	7-2					3	Norepinephrine ↓
TBI traumatic brain injury, *SAH* subarachnoid hemorrhage, *AIS* acute ischemic stroke	8-1	F	55	SAH	14	3	Norepinephrine ↓, Phenylephrine ↓
	8-2					3	Vasopressin ↓

Table 2 ΔMAP, ΔCPP, rCBF$_{XeCT}$, and rCBF$_{DCS}$

No.	Blood pressure, mmHg		Left CBF$_{XeCT}$, mL/100 g/min		Right CBF$_{XeCT}$, mL/100 g/min		Left rCBF, %		Right rCBF, %	
	ΔMAP	ΔCPP	CBF$_{BL}$	CBF$_{IN}$	CBF$_{BL}$	CBF$_{IN}$	XeCT	DCS	XeCT	DCS
1	−35	−33	53.5	32.2	63.2	45.1	−39.8	−41.6	−28.7	−14.7
2	−7	−9	57.6	54.2	47.0	46.5	−18.4	4.1	−14.2	−5.5
3	−22	−17	57.1	45.0	**	**	−21.1	−45.0	**	−36.9
4	25	23	38.5	25.9	18.3	27.7	−32.8	−15.4	51.1	**
5	19	20	**	**	**	**	**	−11.2	**	−38.0
6	−17	−18	25.5	21.4	37.9	28.6	−15.8	−21.1	−24.7	−22.2
7-1	−28	−30	60.1	64.0	**	**	6.5	**	**	18.5
7-2	−10	−14	**	**	38.6	35.1	**	39.9	−9.1	20.2
8-1	−17	−10	61.6	64.2	67.5	65.7	4.1	3.2	−2.7	13.9
8-2	−8	−2	86.5	76.7	**	**	−11.3	−5.9	**	7.7

** XeCT or DCS data were not of acceptable confidence for use

Correlation was not found for either ΔHb ($r_s = -0.51$, $P = 0.087$) or ΔTHC ($r_s = 0.41$, $P = 0.193$).

Comparison of rCBF$_{DCS}$ and NIRS Data

rCBF$_{DCS}$ had a moderate correlation with ΔHbO$_2$ ($r_s = 0.59$, $P = 0.011$) and ΔTHC ($r_s = 0.49$, $P = 0.037$), but no correlation was found with ΔHb ($r_s = -0.06$, $P = 0.788$).

Xenon Inhalation Effects on DCS/NIRS

Figure 4 illustrates one patient's reaction to xenon inhalation. rCBF$_{DCS}$ and ΔTHC changed by 10.9% and 2.1μM, respectively, in the left frontal cortex and 6.4% and 1.3 μM, respectively, in the right frontal cortex, while

Fig. 3 Scatter plot illustrating the correlation between rCBF$_{DCS}$ and rCBF$_{XeCT}$ calculated from ROIs drawn under the optical probes. The fit line has a slope of 1.1 and an offset of 9.3%

MAP increased by 16 mmHg. Such responses observed among the cohort were heterogeneous, and, as a result, they were not significant in the population as a whole ($2.6\% \pm 11.5\%$, $P = 0.191$) with a range of −21.3% to +29.2% relative to baseline. ΔHbO$_2$ ($0.1\ \mu M \pm 1.9\ \mu M$, $P = 0.853$) and ΔTHC ($0.4\ \mu M \pm 1.4\ \mu M$, $P = 0.089$) varied similarly, while ΔHb increased ($0.4\ \mu M \pm 1.0\ \mu M$, $P = 0.035$).

Discussion

In this preliminary study, the feasibility for noninvasive continuous bedside CBF and oxygenation monitoring in the neurocritical care unit using a hybrid optical device was demonstrated. Importantly, DCS/NIRS monitoring of frontal cortical microvascular hemodynamics was performed noninvasively across a range of patients without requiring transport outside the neurointensive care unit. Only frontal epidural or subdural hemorrhages with large enough absorbance to prevent photon detection posed a barrier to the optical signal. DCS measurements of changes in relative CBF correlated well with changes in CBF measured by a well-established, low-throughput technique: stable xenon-enhanced CT. In addition, significant correlations between DCS measurements of rCBF and NIRS measurements of ΔHbO$_2$ and ΔTHC were demonstrated. The association between ΔHbO$_2$ and rCBF$_{XeCT}$ only bordered significance ($P = 0.053$), while no correlation was found for ΔTHC or ΔHb with rCBF$_{XeCT}$.

DCS has not been previously validated in critically brain-injured patients. XeCT is one method used to assess CBF in these patients, with the advantage of providing quantitative CBF measurements and coverage through much of brain parenchyma. However, XeCT requires
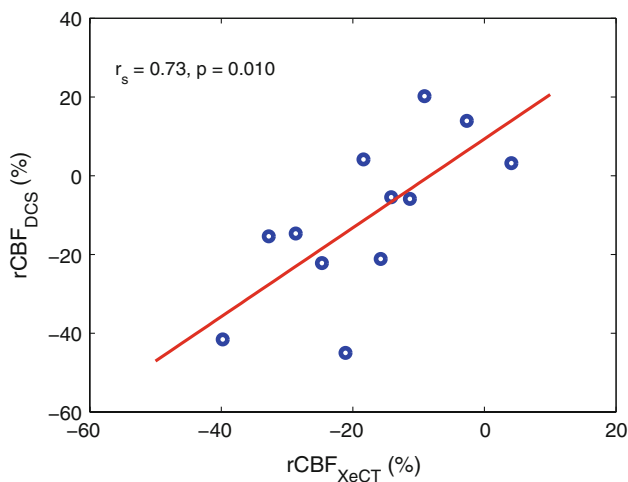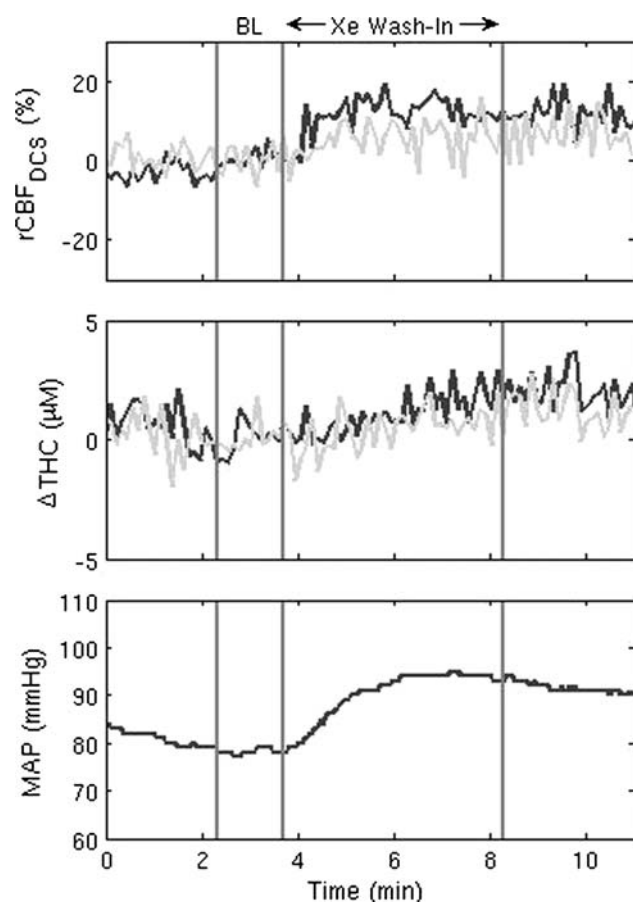
Fig. 4 Example of xenon-enhanced flow activation. *Vertical lines* indicate the following marks: beginning of baseline CT scan (BL), xenon gas washing in, and lastly end of xenon-CT scan. Measurements from the left and right frontal optical probes are indicated by light gray and dark gray lines, respectively. Once xenon begins to wash in, $rCBF_{DCS}$ in both hemispheres begins to increase (*top panel*) and elevated CBF is maintained throughout the duration of the scan. ΔTHC increases in both cerebral hemispheres during the scan (*middle panel*), with a concurrent rise in MAP (*bottom panel*)

exposure to ionizing radiation and cannot provide continuous or even frequent CBF measurements. The good correlation between DCS- and XeCT-measured CBF in this study suggests that DCS may therefore complement existing perfusion imaging techniques by providing continuous, bedside monitoring of CBF in specific cortical ROIs.

As a secondary aim, we examined the correlations between changes in NIRS parameters (ΔHbO$_2$, ΔHb, and ΔTHC) and changes in CBF, as determined by both DCS and XeCT. NIRS assessment of ΔHbO$_2$ is sometimes used as a surrogate of CBF. In this study, we found moderate correlation with $rCBF_{DCS}$ but not with $rCBF_{XeCT}$. One explanation for this finding is simply that more data were available to compare DCS to NIRS than to compare XeCT to NIRS (due to low confidence images from XeCT). The small number of patients was the main limitation of the study, and may have introduced a bias. However,

perturbations in cortical metabolic rate, ICP, arterial inflow, or venous drainage may also complicate the relationship between ΔHbO$_2$ and CBF in neurocritical care patients. Our findings suggest that direct measurements of CBF using DCS are superior to NIRS surrogates and will enhance the diagnostic specificity of transcranial optical monitoring.

Both DCS and NIRS detected the effects of xenon inhalation on CBF and oxygenation. This well-documented phenomenon ("xenon-enhanced flow activation") occurs with the inhalation of stable xenon. As an inert gas, xenon is an anesthetic in high concentrations (70%) [26]. Horn et al. [27] observed xenon-enhanced flow activation in a brain-injured population (using thermal diffusion flowmetry) and demonstrated variability in the magnitude of CBF response (−29% to +44% relative to baseline) that was similar to the variability detected by DCS (−21.3% to +29.2% relative to baseline). Studies by Giller et al. and Hartmann et al. recorded a heterogeneous response in blood velocity and flow even in a healthy cohort [28, 29]. To our knowledge, there are no prior studies employing optics to investigate the effects of xenon inhalation on oxygenation. Examination of the full time-course of CBF throughout XeCT scans could improve the accuracy of the CBF map, but calculations of a simulated 35–45% CBF increase due to xenon-enhanced flow activation yield only a minor 3–5% enhancement in calculated flow as most of the calculations are completed prior to the onset of flow activation [30, 31]. Thus, despite inducing changes in CBF during xenon gas inhalation, the resulting enhancement or reduction in calculated CBF is small compared to errors due to CT noise, motion artifacts, etc.

Like NIRS, DCS has several clinical limits. Light penetration depth is only a few centimeters due to light attenuation by tissue. In the present application, flow measurements were limited to near the surface of the cerebral cortex. In addition, optical data could not be resolved in the presence of underlying extra-axial hemorrhage. Edema directly beneath the optical probes may also prevent signal detection when light absorption is high. Furthermore, since DCS detects changes in CBF more reliably than absolute blood flow. Thus, measurements during a baseline period must be obtained prior to long-term monitoring. Development of an absolute measure of CBF_{DCS} is an area of active research, although arguably, trends in CBF may be more clinically relevant since absolute healthy/ischemic thresholds remain unclear [32–34].

DCS is also limited by the fact that it is a local measure of CBF, and each source–detector pair is only able to probe a region of several cubic centimeters in size. However, multiple probe pairs could be strategically placed with the guidance of CT or MRI to provide continuous monitoring

of the most clinically relevant areas of the brain. Continuous noninvasive CBF measurements in multiple regions could be generated using DCS with significantly less morbidity than using multiple intracerebral monitors.

The good correlation between DCS and XeCT observed in this pilot study provides support for further evaluation of the clinical utility of DCS. Given the dynamic, evolving, and heterogeneous nature of intracranial pathology in brain-injured patients, continuous CBF monitoring may provide the neurointensivist with an important tool for early detection of secondary injury. Since CBF reductions often precede the onset of new clinical symptoms and infarction, DCS monitoring has the potential to detect changes in cerebrovascular physiology while ischemic changes are still reversible. In addition, the configuration of hybrid instrumentation with NIRS would provide comprehensive assessment of cortical blood flow and oxygenation using a single device and the same probes. Additional studies are warranted to assess the utility of DCS/NIRS for neurocritical care, such as by correlating long-term DCS/NIRS measurements of cerebrovascular hemodynamics with patient outcome.

References

1. Waydhas C. Intrahospital transport of critically ill patients. Crit Care. 1999;3:R83–9.
2. Evans DH, McDicken WN. Doppler ultrasound: physics, instrumentation, and signal processing. 2nd ed. Chichester, NY: Wiley; 2000.
3. Vajkoczy P, Roth H, Horn P, et al. Continuous monitoring of regional cerebral blood flow: experimental and clinical validation of a novel thermal diffusion microprobe. J Neurosurg. 2000; 93:265–74.
4. Kirkpatrick PJ, Smielewski P, Czosnyka M, Pickard JD. Continuous monitoring of cortical perfusion by laser Doppler flowmetry in ventilated patients with head injury. J Neurol Neurosurg Psychiatry. 1994;57:1382–8.
5. Reinhard M, Wehrle-Wieland E, Grabiak D, et al. Oscillatory cerebral hemodynamics—the macro- vs. microvascular level. J Neurol Sci. 2006;250:103–9.
6. Boas DA, Campbell LE, Yodh AG. Scattering and imaging with diffusing temporal field correlations. Phys Rev Lett. 1995;75: 1855–8.
7. Maret G, Wolf PE. Multiple light-scattering from disordered media—the effect of Brownian-motion of scatterers. Z Phys B Con Mat. 1987;65:409–13.
8. Pine DJ, Weitz DA, Chaikin PM, Herbolzheimer E. Diffusing-wave spectroscopy. Phys Rev Lett. 1988;60:1134–7.
9. Villringer A, Chance B. Non-invasive optical spectroscopy and imaging of human brain function. Trends Neurosci. 1997;20: 435–42.
10. Hillman EMC. Optical brain imaging in vivo: techniques and applications from animal to man. J Biomed Opt. 2007;12(5): 051402-1–28.
11. Durduran T, Zhou C, Edlow BL, et al. Transcranial optical monitoring of cerebrovascular hemodynamics in acute stroke patients. Optics Express. 2009;17:3884–902.
12. Kim MN, Durduran T, Edlow BL, et al. Healthy aging alters the hemodynamic response to orthostatic stress. Stroke. 2008;39:715.
13. Zhou C, Eucker SA, Durduran T, et al. Diffuse optical monitoring of hemodynamic changes in piglet brain with closed head injury. J Biomed Opt. 2009;14(3):034015-1–11.
14. Pindzola RR, Yonas H. The xenon-enhanced computed tomography cerebral blood flow method. Neurosurgery. 1998;43:1488–92.
15. Yonas H, Pindzola RR, Johnson DW. Xenon/computed tomography cerebral blood flow and its use in clinical management. Neurosurg Clin N Am 1996;7:605.
16. Kety SS. The theory and applications of the exchange of inert gas at the lungs and tissues. Pharmacol Rev. 1951;3:1–41.
17. Durduran T, Yu GQ, Burnett MG, et al. Diffuse optical measurement of blood flow, blood oxygenation, and metabolism in a human brain during sensorimotor cortex activation. Optics Lett. 2004;29:1766–8.
18. Boas DA. Diffuse photon probes of structural and dynamical properties of turbid media: theory and biomedical applications. PhD thesis, University of Pennsylvania; 1996.
19. Duncan A, Meek JH, Clemence M, et al. Measurement of cranial optical path length as a function of age using phase resolved near infrared spectroscopy. Pediatr Res. 1996;39:889–94.
20. Boas DA, Yodh AG. Spatially varying dynamical properties of turbid media probed with diffusing temporal light correlation. J Opt Soc Am A. 1997;14:192–215.
21. Cheung C, Culver JP, Takahashi K, Greenberg JH, Yodh AG. In vivo cerebrovascular measurement combining diffuse near-infrared absorption and correlation spectroscopies. Phys Med Biol. 2001;46:2053–65.
22. Gur D, Yonas H, Good WF. Local cerebral blood flow by xenon-enhanced CT: current status, potential improvements, and future directions. Cerebrovasc Brain Metab Rev. 1989;1:68–86.
23. Obrist WD, Thompson HK, Wang HS, Wilkinson WE. Regional cerebral blood-flow estimated by xenon-133 inhalation. Stroke. 1975;6:245–56.
24. Meyer JS, Hayman LA, Yamamoto M, Sakai F, Nakajima S. Local cerebral blood-flow measured by Ct after stable xenon inhalation. Am J Roentgenol. 1980;135:239–51.
25. Zhang Z. Reliability and error analysis on xenon/CT CBF. Keio J Med. 2000;49(Suppl 1):A29–32.
26. Cullen SC, Gross EG. The anesthetic properties of xenon in animals and human beings, with additional observations on krypton. Science. 1951;113:580–2.
27. Horn P, Vajkoczy P, Thome C, Muench E, Schilling L, Schmiedek P. Xenon-induced flow activation in patients with cerebral insult who undergo xenon-enhanced CT blood flow studies. Am J Neuroradiol. 2001;22:1543–9.
28. Hartmann A, Dettmers C, Schuier FJ, Wassmann HD, Schumacher HW. Effect of stable xenon on regional cerebral blood-flow

and the electroencephalogram in normal volunteers. Stroke. 1991;22:182–9.

29. Giller CA, Purdy P, Lindstrom WW. Effects of inhaled stable xenon on cerebral blood-flow velocity. Am J Neuroradiol. 1990;11:177–82.

30. Obrist WD, Zhang ZH, Yonas H. Effect of xenon-induced flow activation on xenon-enhanced computed tomography cerebral blood flow calculations. J Cereb Blood Flow Metab. 1998;18:1192–5.

31. Good WF, Gur D. Xenon-enhanced CT of the brain—effect of flow activation on derived cerebral blood-flow measurements. Am J Neuroradiol. 1991;12:83–5.

32. Sorensen AG. What is the meaning of quantitative CBF? Am J Neuroradiol. 2001;22:235–6.

33. Steiner LA, Andrews PJ. Monitoring the injured brain: ICP and CBF. Br J Anaesth. 2006;97:26–38.

34. Grandin CB, Duprez TP, Oppenheim C, Peeters A, Robert AR, Cosnard G. Which MR-derived perfusion parameters are the best predictors of infarct growth in hyperacute stroke? Comparative study between relative and quantitative measurements. Radiology. 2002;223:361–70.